ELSEVIER

Talanta 54 (2001) 953–962

Talanta

www.elsevier.com/locate/talanta

Simultaneous determination of organotin compounds by hydride generation–gas phase molecular absorption spectrometry

J. Sanz-Asensio *, M.T. Martínez-Soria, M. Plaza-Medina, M. Pérez Clavijo

Department of Chemistry (Analytical Chemistry), University of La Rioja, Logroño-La Rioja Spain

Received 13 October 2000; received in revised form 12 February 2001; accepted 20 February 2001

Abstract

This study describes the determination of ternary mixtures of dimethyltin chloride (DMT), trimethyltin chloride (TMT) and monobutyltin chloride (BT) by hydride generation–gas phase molecular absorption spectrometry and the application of different chemometric methods: principal components regression (PCR) and partial least squares (PLS). The two methods are applied to the absorption spectra of mixtures of DMT, TMT and BT. Two different experimental designs are tested for the mixtures, a triangular design and a central composite design. The models obtained from the triangular design offer the best prediction results. The effects of the number of working wavelengths and the number of factors included in the calibration model is studied and a different behaviour is seen for each compound and calibration model. The methods are applied to the analysis of artificial aqueous samples containing different concentrations of DMT, TMT and BT species. No significant differences are observed between the calibration models investigated.

Keywords: Hydride generation; Gas phase molecular absorption spectrometry; Organotin compounds

1. Introduction

Analytical applications of Gas Phase Molecular Absorption Spectrometry (GPMAS) have been independently developed by Syty [1] and by Cresser [2] since 1973. The technique is based on the measurement of the absorption of molecular species in the gas phase, generated at room temperature. Its application has focused on sulphur compounds [3], nitrogenated compounds [4], halides [5], covalent hydride volatiles [6] and more recently, arsenic and tin organo-metals [7,8].

A variety of analytical techniques have been described for the speciation of organotin compounds. Many of these are based on separation via high performance liquid–liquid chromatography (HPLC) [9] or more often using gas chromatography (GC) [10]. The derivatisation by hydride generation with sodium tetrahydroborate (III) [11], sodium tetraethyl borate [12] and alkylation by Grignard reagents [13] are the most

* Corresponding author. Fax: +34-941-299621.
E-mail address: jesus.sanz@dq.unirioja.es (J. Sanz-Asensio).

0039-9140/01/$ - see front matter
PII: S0039-9140(01)00365-4

commonly used methods for the analysis of these compounds by conversion to volatile species. Several detection techniques have been coupled to GC and HPLC for the determination of derivatised organotin compounds. These include atomic absorption spectrometry (AAS) [14], atomic emission spectrometry (AES) [15], mass spectrometry (MS) [16], flame photometric detection (FPD) [17] and microwave-induced plasma atomic emission spectrometry (MIP-AES) [18]. Multivariate calibration is an alternative for the speciation of analytical species. Multivariate methods such as multiple linear regression (MLR) [19], principal component regression (PCR) [20] and partial least squares regression (PLSR) [21] are widely used for simultaneous determination with multivariate data, such as those provided by UV/Visible absorption [22], infrared [23] or fluorescence [24].

In many multicomponent determinations by spectroscopy, measurements from many spectral wavelengths are non-informative or are difficult to incorporate into a model because of nonlinearities. In these applications, it is appropriate to refine the model through the elimination of the variables which give non-useful information or no new information in the case of highly correlated data. Several variable selection methods have been used, such as stepwise regression and ridge regression [25], neural networks [26] or genetic algorithms [27]. In this work, the wavelength selection for spectrophotometric data analysis by PCR and PLS methods is based on the principal bw coefficients [28,29].

The aim of this study is the simultaneous determination of dimethyltin chloride, trimethyltin chloride and monobutyltin chloride using the generation of the corresponding hydrides, carried out by continuous addition of the reducing agent and subsequent determination by GPMAS and the application of PCR and PLS multivariate methods. The individual study of these species has already been described in previous papers. Two calibration matrix designs were used to statistically maximise the information content of the spectra.

2. Experimental

2.1. Apparatus

All measurements were made with a Hewlett-Packard (HP) model 8451 diode-array spectrophotometer equipped with HP 98155A keyboard, HP 9121 disk drive for bulk data storage, HP Thinkjet printer and an HP 7475A graphics plotter. A Hellma 174QS 1 cm quartz flow cell was used, together with a Peristaltic pump (Cole Parmer Instrument Co. 7554-20), an Agitamatic Heidolph MR 3003 with platinum probe, a Mettler PJ 3600 Delta Range, a Dewar (2 l) Dilvac and a Schott ISO 250/1000 ml generator flask. The generation scheme and procedure system are already described in previous papers [30].

2.2. Reagents

Stock solutions of organotin compounds were prepared of 1000 μg ml^{-1} in Sn as follows: dimethyltin chloride (DMT), $C_2H_6SnCl_2$ from Aldrich (Sigma-Aldrich, USA) dissolved in double-distilled water, trimethyltin chloride (TMT), C_3H_9SnCl from Aldrich dissolved in double-distilled water and monobutyltin trichloride (BT), $C_4H_9SnCl_3$ from Aldrich dissolved in double-distilled water. Working standards were prepared by serial dilution of the stock solutions with water, immediately before use. Aqueous solutions of sodium tetrahydroborate (III), $NaBH_4$ from Carlo Erba (Milan, Italy) were prepared immediately prior to use. Hydrochloric acid (37%, 1.186 g ml^{-1}) was RPE grade from Carlo Erba. Working solutions were prepared daily by diluting the concentrated solutions with water. All water used was double-distilled. The Calcium chloride was dried granular RE grade from Carlo-Erba. The carrier gases were nitrogen and hydrogen (C-50 Carburos Metálicos).

2.3. Experimental design of the calibration matrix

The hydrides of DMT, TMT and BT were made by adding a sodium tetrahydroborate (III) solution to a volume of the acidified standard

solution. The hydrides generated absorb in the UV region. The generation scheme and procedure system were as already described in previous papers. Fig. 1 shows the absorbance spectra of dimethyltin hydride (DMTH), trimethyltin hydride (TMTH) and monobutyltin hydride (BTH). The absorbance spectra were obtained between 190–250 nm, taking absorbance data at 2 nm intervals.

Due to the high overlap between the absorption bands of the three components, the application of two multivariate calibrations methods, principal components regression (PCR) and partial least square regression (PLSR), was evaluated.

Two calibration matrix designs were used to statistically maximise the information content of the spectra. The first was a concentration set corresponding to a 2^3 central composite design with a central point, enabling analysis of five levels of concentration for each of the three analytes. The composition of the calibration mixtures is shown in Table 1. Secondly, a triangular design with a training set of 10 samples was taken. In this design, each component was analysed in six levels. Table 2 shows the composition of the calibration mixtures. Spectral data were converted to ASCII files and subsequently all data processing was performed with the Parvus 3.0 software package [31].

2.4. Determination of the number of factors

An important step in PCR and PLS calibration is the determination of the number of factors to be included in the calibration model. In order to select the number of factors, a cross-validation method, with five deletion groups, was used.

The percentage of explained variance in cross-validation (% EVCV) was used for determination of the optimum dimensionality of the PLS and PCR models. The cross-validation method involves the use of the original calibration set to simulate a validation set. To do this, the calibration set is divided into k deletion groups. PLS and PCR calibrations are then performed after removing the first deletion group and the models are constructed based on the remaining samples in the calibration set. Using the calibration model, the concentration of the samples in the deletion group, left out during calibration, are predicted and this process is repeated k times until all the samples (k deletion group) have been predicted only once.

For each cycle, the PRESS value is calculated (Predicted Residual Error Sum of Squares). The sum of the PRESS values obtained for each cycle gives the total PRESS, which is an estimation of the total sum of squares error expected in the prediction. The explained variance cross-validated (EVCV) after computing F factors is given by:

$$\mathrm{EVCV}(F) = 1 - \frac{\mathrm{PRESS}\ (F)/N}{\text{Initial data variance}}$$

$$\mathrm{PRESS}(F) = \sum_k \sum_i (y_i - \hat{y}_{i_{C(k)}})^2$$

where y_i is the concentration of analyte in the ith sample, $\hat{y}_i$ is the estimated concentration of the analyte by the model with F factors when the kth deletion group is removed, and N is the total number of samples. The EVCV (%) was obtained for each calibration generated with every possible number of factors. The maximum percentage of explained variance in cross-validation is obtained when the PRESS value is minimum, and the number of factors for the maximum EVCV (%) value was selected as optimum.

2.5. Selection of wavelengths for the calibration methods

The choice of wavelengths for model building using PCR and PLS methods is critical to the generation of a robust model with a good predictive ability. For the selection of the optimum wavelength range, the bw coefficients obtained in the regression were selected.

When the calibration data is autoescalated prior to initial PLS or PCR modelling, the regression equation is:

$$Y = X_{\mathrm{aut}} B_{\mathrm{w}} + E$$

where B_{w} is the matrix of bw regression coefficients (indicating they have been obtained from autoescalated data) and E is the matrix of residuals.

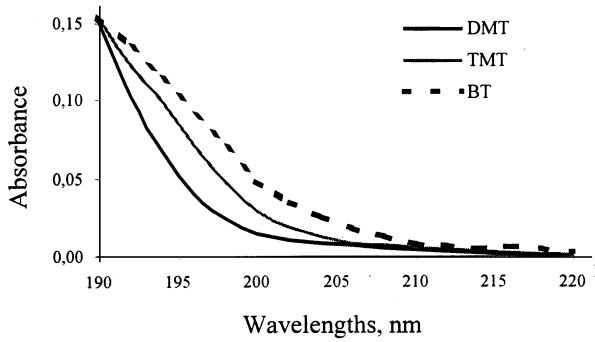

Fig. 1. Absorption spectra of DMTH, TMTH and BTH compounds.

Table 1
Concentration data for the mixtures used in the calibration set corresponding to a central composite design

Samples	DMT (ng ml^{-1})	TMT (ng ml^{-1})	BT (ng ml^{-1})
M1	102.2	35.2	123.8
M2	102.2	35.2	371.4
M3	102.2	98.4	123.8
M4	102.2	97.8	371.4
M5	306.7	35.2	123.8
M6	306.7	35.2	371.4
M7	306.7	97.8	123.8
M8	306.7	97.8	371.4
M9	32.4	66.5	247.6
M10	376.3	66.5	247.6
M11	204.3	13.9	247.6
M12	204.3	119.1	247.6
M13	204.3	66.5	39.4
M14	204.3	66.5	455.8
M15	204.3	66.5	247.6

The bw coefficients can be used directly to choose the principal variables. A large bw coefficient implies a significant X variable, and therefore indicates which variables are dominantly influencing the model. The method makes the assumption that only wavelengths with large bw coefficients are useful for prediction.

This method is based on the calculation of the bw coefficients that correspond to the model with the optimal number of factors, as follows:

- The calibration method was applied to the autoescalated data and the calibration model obtained, with the regression coefficients (bw coefficients). The optimum number of factors for this model was selected using the maximum %EVCV value criterion.
- The bw coefficients that correspond to the model with the optimum number of factors were represented and different levels of bw coefficients were selected, to be greater than a particular value, regardless of sign.
- The calibration models with prior centring data for the selected variables were calculated. For each model the %EVCV value with five deletion groups and the prediction error were calculated. The prediction error was calculated as follows:

$$\text{PE}\ (\%) = \frac{\sqrt{\sum [y_i - \hat{y}_i]^2}}{\sqrt{\sum [y_i]^2}} \times 100$$

where y_i is the standard concentration of analyte in the sample i and $\hat{y}_i$ is the predicted concentration of the analyte in sample i when the sample is in the k deletion group. The model with smallest PE(%) was selected.

Table 2
Concentration data for the mixtures used in the calibration set corresponding to a triangular design

Samples	DMT (ng ml^{-1})	TMT (ng ml^{-1})	BT (ng ml^{-1})
M1	376.3	13.9	39.4
M2	32.4	119.3	39.4
M3	32.4	13.9	455.8
M4	204.3	66.5	39.4
M5	204.3	13.9	247.6
M6	32.4	66.5	247.6
M7	147.9	48.9	178.8
M8	261.0	31.5	108.9
M9	89.7	84.0	108.9
M10	89.7	31.5	31.6

3. Results and discussion

3.1. Optimization of calibration models

Prior to the autoescalation of the data sets, the PCR and PLS calibration models were calculated with different number of factors for both ana-

Table 3
Results obtained in the calculation of calibration methods based on the criterion of the bw coefficients for the selection of wavelengths based on the central composite design

DMT				TMT				BT			
No. V[a]	No. F	%EVCV	PE (%)	No. V	No. F	%EVCV	PE (%)	No. V	No. F	%EVCV	PE (%)
PCR											
6	6	94.73	10.4	5	5	80.65	18.1	7	6	96.21	8.4
12	7	92.22	11.1	11	6	98.25	5.4	12	4	93.34	11.2
21	6	89.97	13.3	21	5	96.64	7.2	21	6	94.51	10.1
PLS											
6	3	90.37	10.8	7	6	99.06	9.7	7	5	93.06	16.3
11	4	92.49	9.6	10	6	99.06	9.7	13	4	94.89	10.1
21	4	90.14	10.3	21	6	97.51	15.8	21	5	94.59	13.3

[a] No. V, number of wavelengths; No. F, number of factors.

Table 4
Results obtained in the calculation of calibration methods based on the criterion of the bw coefficients for the selection of wavelengths based on the central triangular design

DMT				TMT				BT			
No. V[a]	No. F	%EVCV	PE (%)	No. V	No. F	%EVCV	PE (%)	No. V	No. F	%EVCV	PE (%)
PCR											
6	4	95.78	12.9	7	4	72.64	30.8	8	6	95.86	14.0
13	4	95.58	13.2	11	4	82.10	21.5	12	6	96.31	13.2
21	4	93.60	15.9	21	5	99.15	5.4	21	6	99.06	6.7
PLS											
8	6	98.15	8.1	6	4	96.68	10.8	9	6	97.94	9.0
13	5	95.55	12.5	11	4	93.31	12.6	13	6	97.36	9.2
21	5	97.31	9.8	21	4	92.83	13.1	21	6	93.97	13.3

[a] No. V, number of wavelengths; No. F, number of factors.

Table 5
Statistical parameters of the calibration

	PCR			PLS		
	DMT	TMT	BT	DMT	TMT	BT
Central Composite Design						
R^2	0.9939	0.9977	0.9917	0.9931	0.9987	0.9917
RMSD	5.3948	3.9499	5.6327	5.0563	2.8045	5.7012
Triangular Design						
R^2	0.9939	0.9988	0.9987	0.9986	0.9918	0.9985
RMSD	4.5296	3.2258	3.1981	3.1480	4.1871	3.2142

Table 6
Concentration data of the synthetic samples of DMT, TMT and BT

Sample	DMT (ng ml^{-1})	TMT (ng ml^{-1})	BT (ng ml^{-1})
M1	32.4	119.1	108.9
M2	89.7	48.9	123.8
M3	147.9	66.5	247.6
M4	204.3	35.2	178.8
M5	102.2	97.8	455.8

lytes. The optimum number of factors to be included in the calibration models was calculated according to %EVCV criteria. For the PCR algorithm, the optimum number of factors with the central composite design was six for the DMT and BT species and five for the TMT; for the PLS model, the numbers were six factors for the DMT, five factors for the TMT and four for BT. Using the triangular design, four factors were selected for the DMT, five factors for the TMT and six factors for the BT for the PCR model, and six factors for all species with the PLS model.

Fig. 2 shows the bw coefficients versus wavelength for each variable and each calculated model for the calibration matrix, based on the central composite design. Very different profiles can be seen for each of the species when the PCR model was used (Fig. 2A): for DMT, the highest coefficients correspond to the lowest wavelengths; TMT shows more uniform values, from 194 to 208 nm, with maxima at 216 and 218 nm, with lower coefficient values than for those of the remaining two species; the BT showed the highest values in the intermediate wavelength range, from 202 to 212 nm. The profiles obtained using the PLS method (Fig. 2B) were also very different, while giving wavelength ranges similar to those obtained from PCR: low wavelengths with a maximum at 208 nm for the DMT, a range from 194 to 208 nm for the TMT with maxima at 216 and 218 nm, and an intermediate range for the BT species. In this case, it can be seen that the highest coefficient values were obtained for the DMT species.

Fig. 3 shows the bw coefficients versus wavelength for each variable and each calculated

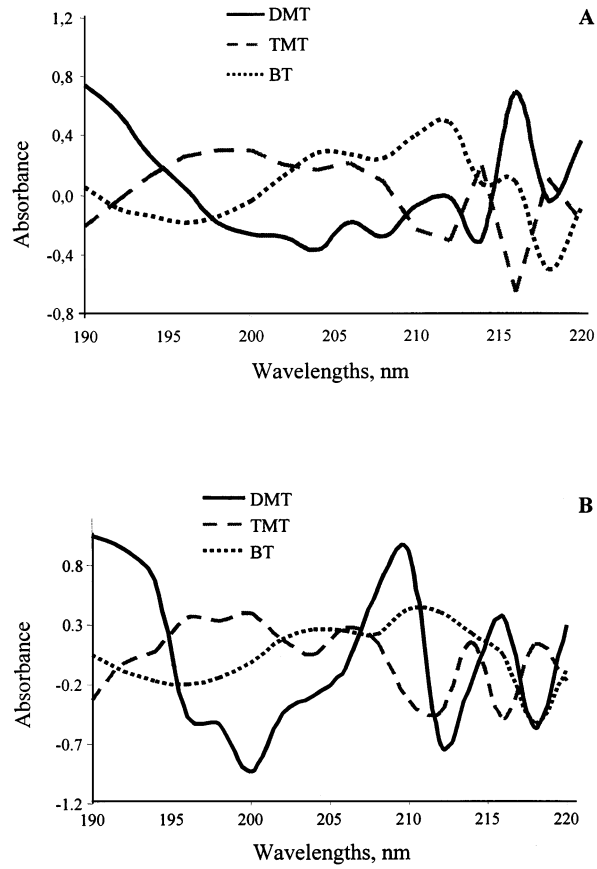

Fig. 2. bw coefficients for the DMT, TMT and BT for (A) PCR model, (B) PLS model based on the central composite design.

model for the calibration matrix based on the triangular design.

Very different profiles are seen for each of the species with either of the two methods. For DMT, the highest coefficients were seen at the lowest wavelengths for the two calibration methods. For TMT, more uniform values were seen, from 196 to 214 nm for the PCR method and a range from 190 to 198 nm and from 204 to 212 nm for the PLS method. The BT showed the highest values in the low wavelength range, with a maximum at 218 nm for the PCR method and intermediate values, from 194 to 222 nm, for the PLS method. In this case, it can be seen that the values of the coefficients are comparable for the three species and are lower than those obtained with the previous design.

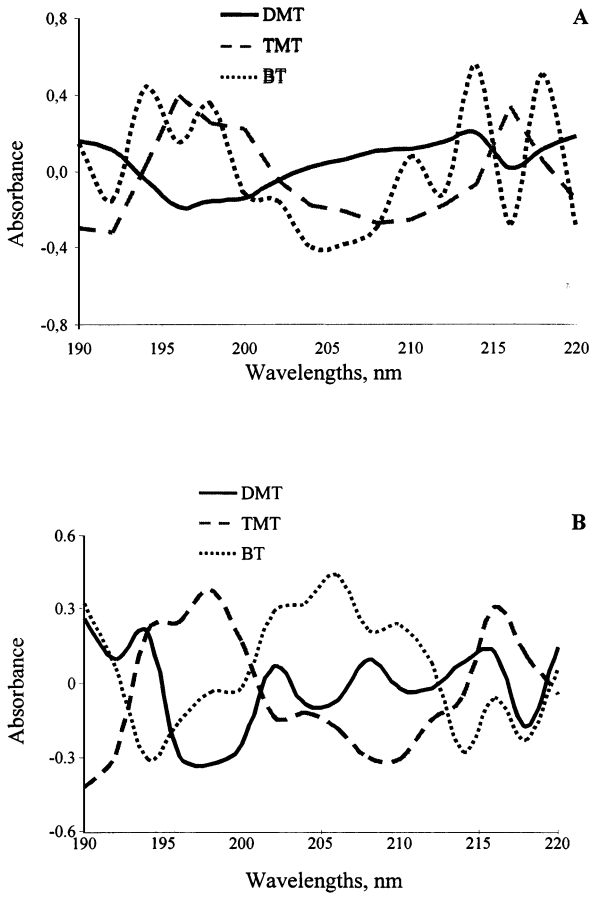

Fig. 3. bw coefficients for the DMT, TMT and BT for (A) PCR model, (B) PLS model based on the triangular design.

In function of the bw coefficient values, different levels of wavelengths were chosen for each component. Three levels of wavelengths were studied for each component and calibration method. For each group and calibration method, the model was calculated, with prior mean centring of the data set, and the values of %EVCV and %PE were obtained. Tables 3 and 4 summarise the values obtained with PCR and PLS models and each calibration matrix with the optimum factor number.

It can be seen that different behaviour was presented for each calibration method obtained with the central composite method. For the PCR model, the %PE was reduced when the number of wavelengths reduced. The best prediction was obtained using six variables for the DMT, eleven variables for TMT and seven for the BT species.

A similar effect was observed for the PLS model. The %PE was reduced for the intermediate range of variables. The best prediction was obtained using 11, 10 and 13 variables for the DMT, TMT and BT species, respectively. In all the selected models, the %EVCV exceeded 90%.

It can be seen that different behaviour was presented for each calibration method obtained with the model based on the triangular design, Table 4. For the PCR model, this needed all the wavelengths for the TMT and BT species, however for the DMT the best prediction was obtained using a reduced number of variables, 6, the same number obtained with the central composite design.

For the PLS model the three compounds showed the best prediction with a reduced number of variables: 8, 6 and 9 for the DMT, TMT and BT respectively. This behaviour is similar to that obtained with the central composite design. The optimum number of factors found for the models derived from the triangular calibration design was practically constant for the various wavelength levels of each species; greater variation was seen between the models obtained from the central composite design, indicating that the triangular design is more robust. Furthermore, it can be seen that the %EVCV values obtained for all the models selected were higher than 95%, a superior result to that obtained from the central composite design.

3.2. Analytical characteristics

With the number of factors and wavelength ranges selected, the calibration models were calculated for all the calibration set. Table 5 shows the root mean square difference (RMSD) and R^2 of the calibration models. The RMSD is an indication of the average error in the analysis

$$\mathrm{RMSD} = \left[1 \Big/ N\sum_{i=1}^{N}(\hat{y}_i - y_i)2 \right]^{0.5}$$

and the square of the correlation coefficient (R^2), an indication of the quality of fit of all the data to a model:

Table 7
Results obtained in the resolution of the artificial mixtures of DMT, TMT and BT

Samples	PCR						PLS					
	DMT		TMT		BT		DMT		TMT		BT	
Central Composite Design												
	Rec (%)	RSD[a] (%)	Rec (%)	RSD[a] (%)	Rec (%)	RSD[a] (%)	Rec (%)	RSD[a] (%)	Rec (%)	RSD[a] (%)	Rec (%)	RSD[a] (%)
M1	126.4	37.5	99.5	1.0	97.8	6.8	112.2	11.1	98.8	1.4	100.9	2.9
M2	98.9	3.6	99.6	3.4	101.9	2.5	101.6	1.5	98.7	5.5	100.6	2.6
M3	99.2	3.3	98.9	3.6	103.1	2.1	96.6	1.9	100.4	2.3	98.4	3.7
M4	100.7	2.7	102.1	3.1	100.6	2.0	100.1	1.0	102.0	1.8	100.5	1.5
M5	106.3	4.7	99.8	0.6	102.2	4.3	102.9	2.8	100.2	1.9	102.7	4.2
Triangular Design												
M1	98.7	4.8	99.9	2.4	101.0	2.5	98.7	7.4	101.0	2.3	98.5	3.0
M2	102.3	4.0	99.6	2.7	97.8	1.3	102.1	2.4	99.8	5.4	99.0	1.4
M3	100.0	1.7	99.3	3.4	99.0	2.3	99.8	1.8	99.1	3.3	101.1	1.2
M4	100.4	1.6	103.4	6.2	98.4	1.3	100.3	2.5	102.1	7.7	101.0	1.0
M5	100.4	1.5	98.8	4.7	100.2	1.1	101.8	6.2	101.5	2.1	99.8	0.4

[a] Mean of three independent determinations.

$$R^2 = 1 - \sum_{i=1}^{N}(y_i - \hat{y}_i)^2 \Big/ \sum_{i=1}^{N}(y_i - \bar{y})^2$$

where y_i is the standard concentration of analyte in the sample i, $\hat{y}_i$ is the estimated concentration of the analyte in the sample i, $\bar{y}$ the mean of standard concentrations and N the total number of samples.

It can be seen that there are significant differences between the values found for RMSD and R^2 with the two calibration models; those obtained from the triangular design gave better calibration parameters. Within the models, the parameters obtained from the PCR and PLS were similar.

The proposed calibration models allow the quantitative resolution of ternary mixtures of DMT, TMT and BT compounds. In order to evaluate the predictive ability of each calibration model, the obtained models were applied to the molecular absorption spectra of artificial aqueous samples and predictions were obtained. Tables 6 and 7 show the real and predicted values for the DMT, TMT and BT, applying the two models obtained from each calibration design to one set of samples.

It can be seen that all the models allow the obtaining of quantitative results in the simultaneous determination of DMT, TMT and BT by HG–GPMAS, and that those obtained via the triangular calibration matrix gave better predictions.

4. Conclusions

The use of a diode-array molecular absorption spectrometer as the detector allows the obtaining of the spectra of generated volatiles over a wide wavelength range. This permits the application of multivariate calibration methods.

The calibration methods applied permit the simultaneous determination by multivariate calibration of dimethyltin chloride, trimethyltin chloride and monobutyltin chloride by HG-GPMAS. Two calibration designs were used to maximise the information contained in the spectra, a triangular design and a central composite design; the study demonstrates that the best results were found with the former.

The results obtained from the application of the wavelength selection model, used in the calculation of the calibration model, allowed corroboration that this stage is critical; it demonstrated that for each compound, there is a determined range of variables which allow for the construction of a robust model and which gives optimum predictive capacity. In many cases, this range is different to the initial one used.

Acknowledgements

The authors would like to thank the University of La Rioja for the financial support given to carry out this research. The authors also want to thank the CAICYT (Project No. 541-A783). Margarita Pérez Clavijo, would like to thank the MEC for the FPI grant.

References

[1] A. Syty, Anal. Chem. 45 (1973) 1744.
[2] M.S. Cresser, P.J. Isaccson, Talanta 23 (1976) 885.
[3] A. Safavi, B. Haguigui, Talanta 44 (1997) 1009.
[4] J. Sanz, S. de Marcos, O. Muro, J. Galbán, Mikrochim. Acta 110 (1993) 193.
[5] M.A. Firestone, M.L. Dietz, A. Syty, Anal. Lett. 18 (1985) 985.
[6] J. Sanz, S. Cabredo, J. Galbán, Talanta 46 (1998) 631.
[7] J. Sanz-Asensio, M.T. Martínez-Soria, M. Plaza-Medina, M. Pérez-Clavijo, Anal. Chim. Acta 381 (1999) 331.
[8] J. Sanz, M. Pérez, M.T. Martínez, M. Plaza, Talanta 51 (2000) 849.
[9] A. Mazucottelli, R. Freche, L. Zaratin, P. Rivaro, Analyst 120 (1995) 1171.
[10] C. Bancon-Montigny, G. Lespes, M. Pontin-Gautier, Analyst 124 (1999) 1265.
[11] H. Narasaki, Anal. Sci. 14 (1998) 857.
[12] F.M. Martin, O.F.X. Donard, Fresenius J. Anal. Chem. 351 (1995) 230.
[13] T. Suzuki, K. Kondo, M. Uchiyama, M. Murayama, J. Agric. Food Chem. 47 (1999) 3886.
[14] S. Dadfarnia, K.C. Thompson, G. Hoult, JAAS 9 (1994) 7.
[15] I.R. Pereiro, A. Wasik, R. Lobinski, Fresenius J. Anal. Chem. 363 (1999) 460.
[16] H. Tao, R.B. Rajendran, T. Nakazato, M. Tominaga, A. Miyasaki, Anal. Chem. 71 (1999) 4211.
[17] M.J. Waldock, M.E. Waite, Appl. Organomet. Chem 8 (1994) 649.

[18] I. Rodriguez Pereiro, A. Wasik, R. Lobinski, J. Chromatogr. A 795 (1998) 359.
[19] C. Demir, R.G. Brereton, Analyst 123 (1998) 181.
[20] T. Galeano Díaz, M.I. Acedo Valenzuela, F. Salinas, Fresenius J. Anal. Chem. 350 (1994) 692.
[21] A. Espinosa Mansilla, F. Salinas, M. del Olmo, I. de Orbe Payá, Applied Spectrosc. 50 (1996) 449.
[22] F. Martin, M. Otto, Fresenius J. Anal Chem. 352 (1995) 451.
[23] Z. Bouhsain, S. Garrigues, M. de la Guardia, Analyst 121 (1996) 1935.
[24] C. Leal, M. Granados, J.L. Beltrán, R. Compañó, M.D. Prat, Analyst 122 (1997) 1293.
[25] D.C. Montgomery, E.A. Peck, Introduction to Linear Regression Analysis, Wiley, New York, 1982.
[26] J. Wikel, E. Dow, Boorg. Med. Chem. Lett. 3 (1993) 645.
[27] D. Jouan-Rimbaud, D.L. Massart, R. Leardi, O.E. de Noord, Anal. Chem. 67 (1995) 4295.
[28] A. Garrido Frenich, D. Jouan-Rimbaud, D.L. Massart, S. Kuttatharmmakul, M. Martínez Galera, J.L. Martínez Vidal, Analyst 120 (1995) 2787.
[29] S.D. Osborne, R.B. Jordan, R. Künnemeyer, Analyst 122 (1997) 1631.
[30] J. Sanz, M. Pérez, M.T. Martínez, M. Plaza, Talanta 50 (1999) 149.
[31] Parvus, M. Forina, S. Lanteri, C. Armanino, R. Leardi, G. Drava, Universitá degli Studi di Genova (invoice No 18/5002).